

Time delay by primordial density fluctuations: its biasing effect on the observed mean curvature of the Universe

Richard Lieu¹ and Jonathan P.D. Mittaz²

¹*Department of Physics, University of Alabama, Huntsville, AL 35899.*

²*Cooperative Institute for Climate Studies, ESSIC, University of Maryland
2NOAA/NESDIS, Camp Springs, Maryland.*

ABSTRACT

In this paper we specifically studied one aspect of foreground primordial matter density perturbations: the relative gravitational time delay between a pair of light paths converging towards an observer and originating from two points on the last scattering surface separated by the physical scale of an acoustic oscillation. It is found that time delay biases the size of acoustic oscillations *systematically* towards smaller angles, or larger harmonic numbers ℓ , i.e. the mean geometry as revealed by CMB light becomes that of an open Universe if $\Omega = 1$. Since the effect is second order, its standard deviation $\delta\ell/\ell \sim (\delta\Phi)^2$ where $(\delta\Phi)^2 \sim 10^{-9}$ is the normalization of the primordial matter spectrum $P(k)$, the consequence is too numerically feeble to warrant a re-interpretation of WMAP data. If, however, this normalization were increased to $\delta\Phi \gtrsim 0.01$ which is still well within the perturbation limit, the shift in the positions of the acoustic peaks would have been substantial enough to implicate inflationary Λ CDM cosmology. Thus Ω is not the only parameter (and by deduction inflation cannot be the only mechanism) of relevance to the understanding of *observed* large scale geometry. The physics that explains why $\delta\Phi$ is so small also plays a crucial role, but since this is a separate issue independent of inflation, might it be less artificial to look for an alternative solution to the flatness problem altogether?

Subject headings:

1. Introduction

Among the so-called ‘secondary’ physical mechanisms that re-process the CMB anisotropy, such as gravitational lensing, time delay, and the Sunyaev-Zel’dovich effect, time delay by foreground inhomogeneities in the matter distribution appears to be investigated least. In

the recent period a detailed treatment of the problem was provided by Hu & Cooray (2001, hereafter HC01), although the general framework for calculating gravitational perturbation effects on the CMB as published in the review of CMB lensing by Lewis & Challinor (2006) could also be employed to carry the study further.

In HC01 the authors found an infra-red logarithmic divergence in the variance of the *absolute* (or total) time delay along a randomly chosen direction to the LSS. They ‘renormalized’ this infinity by subtracting the contribution from the ‘monopole’ term of the matter power spectrum, corresponding to the removal of a constant uniformly across the sky. Nevertheless, the remaining (finite) quantity still carries the divergence trend. More precisely the variance is dominated by long wavelength fluctuations, prompting HC01 to consider it as an effect of very large coherence length, $\Delta\ell \approx 2$ which does not affect our interpretation of the CMB anisotropy, because the net outcome is simply a gentle and arbitrary distortion of the spherical shape of the LSS, completely negligible over the size of one (or a few) cycles of CMB acoustic oscillations.

The coherence length inferred by HC01 should be viewed with some caution, however, because the large delay excursion of ~ 1 Mpc/c calculated there, which involved only the *zeroth* order term, the path integral of the perturbing potential itself, stems from the part of the matter power spectrum which carries the scale-invariant Harrison-Zel’dovich dependence $P(k) \sim k$, i.e. there is a danger that the large coherence length may simply be due to the infra-red divergence of the variance rather than any genuine physical scale in the matter spectrum. To find the coherence length of relevance to the question of CMB anisotropy distortion, it is necessary to pursue the perturbation expansion to the next two orders. Not only are both results free from divergences, but also it is only through a comparison of these two terms that the true coherence scale for variations in the *relative* delay between two light paths separated by a small angle θ would become transparent. We shall find that this scale is defined by a physically significant parameter, viz. the characteristic wavenumber at which departures of $P(k)$ from the Harrison-Zel’dovich behavior occurs for the first time. The consequence is that appreciable distortion of the LSS radius, with both amplitudes and wavelengths on par with the dimension of the primary acoustic oscillations at the time of last scattering, can exist in principle.

2. Perturbation in the gravitational potential from the 2dFGRS/WMAP1 power spectrum of primordial matter

Although in the $k \rightarrow 0$ limit the matter power spectrum has the form $P(k) \sim k$, the behavior of $P(k)$ at large k is more complicated than an exponential cutoff. It is possible,

however, to break down *any* general $P(k)$ into constituent terms, each of the form $a_i k e^{-b_i k}$, and sum up the time delay fluctuation contributions from all the terms, because $P(k)$ has the meaning of a variance, i.e. it too is additive. We may therefore write

$$P(k) = A(a_1 k e^{-b_1 k} + a_2 k e^{-b_2 k} + \dots), \text{ with } \sum_i a_i = 1. \quad (1)$$

This empirical representation of $P(k)$ is not the same as the more commonly used ones (e.g. Efstathiou, Bond, and White 1992) but, as shall be seen in section 3, the exponential form reveals coherent length scales of foreground effects in a transparent way; in any case, provided our formula for $P(k)$ fits the observational data (see below) the detailed structure of the terms used to model the spectrum is of no significance.

The resulting value of A in Eq. (1) that we shall obtain is

$$A = 3.276 \times 10^7 \text{ Mpc}^4, \quad (2)$$

and leads, by Eq. (A-6), to

$$\delta\Phi \approx 3 \times 10^{-5}, \quad (3)$$

for a $\Omega_m = 0.3$, $\Omega_\Lambda = 0.7$, and $h = 0.7$ cosmology (Bennett et al 2003, Spergel et al 2007). This agrees well with the CMB temperature modulation of $3\delta T/T$ at small k as measured by WMAP (see e.g. Bennett et al 2003), as it ought to, because from Eq. (A-5)

$$(\delta\Phi)^2 = \lim_{k \rightarrow 0} \frac{d\Phi_k^2}{d\ln k} = \lim_{k \rightarrow 0} \left(\frac{3\delta T_k}{T_k} \right)^2, \quad (4)$$

where the final step is explained in the material around Eq. (18.14) of Peacock (1999). The consistency between $\delta\Phi$ as derived from our $z = 0$ matter spectrum and the large scale CMB anisotropy re-assures us that any corrections we ignored, such as the effect of vacuum domination at $z \lesssim 0.3$, are indeed minor.

If $P(k)$ has the simple form involving only the first term of Eq. (1) with $a_1 = 1$, we may work out from Eq. (A-5) the correlation function for the perturbing Newtonian potential Φ that arises from the linear growth of primordial density contrasts, as

$$\langle \Phi(\mathbf{r})\Phi(\mathbf{r}') \rangle = \frac{9\Omega_m^2 H_0^4}{32\pi^3} \int \frac{d^3\mathbf{k}}{k^4} e^{i\mathbf{k}\cdot(\mathbf{r}-\mathbf{r}')} P(k) = \frac{(\delta\Phi)^2}{4\pi} \int \frac{d^3\mathbf{k}}{k^3} e^{i\mathbf{k}\cdot(\mathbf{r}-\mathbf{r}')} e^{-bk}, \quad (5)$$

where Φ is assumed to be time-independent and Gaussian distributed, and in the final step use was made of Eqs. (A-4) and (A-6). If $P(k)$ is given by the full Eq. (1) instead, then the rightmost side of Eq. (5) will be a sum of similar terms, each carrying the exponent b_i and with $(\delta\Phi)^2$ replaced by $a_i(\delta\Phi)^2$.

Implementing now the observed power spectrum, the most up to date data are from the 2dFGRS galaxy survey (Cole et al 2005) after they are deconvolved and aligned with the WMAP1 normalization by setting the σ_8^2 parameter to $\sigma_8^2 = 0.74$ (Sanchez et al 2006). We found that the resulting dataset can adequately be fitted with a function for $P(k)$ of the form given by Eq. (1) and involving three exponential terms, with the value of A as already quoted in Eq. (2) and the values of a_i and b_i ($i = 1,2,3$) as shown in Table 1. This best-fit spectrum, which closely follows that of WMAP1's Λ CDM model (Spergel et al 2003) is plotted in Fig. 1.

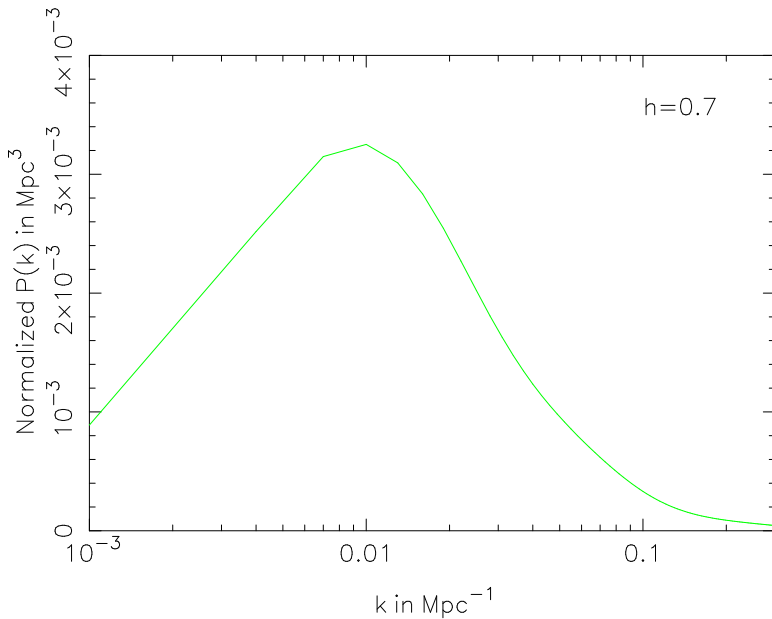


Fig. 1.— The best $P(k)$ model of the WMAP1 normalized 2dFGRS data as given by Eq. (1) with $A = 1$ and the remaining parameters as shown in Table 1. The Hubble constant assumed is $h = 0.7$.

3. Cosmological time delay variation from primordial density contrasts

We proceed towards calculating the excursion in time delay along two light paths of equal lengths. Our starting point is a flat Universe having its average density at the critical value, as required by the WMAP observations (Bennett et al 2003, Spergel et al 2007). We employ Cartesian comoving coordinates and the conformal time coordinate η , so that in a perturbed flat FRW space light propagates along the null geodesics of the metric

$$ds^2 = (1 + 2\Phi)d\eta^2 - (1 - 2\Phi)(dx^2 + dy^2 + dz^2), \quad (6)$$

as though the expansion factor $a(\eta)$ plays no role. Let light signals arrive at the observer's origin from a source at $(x, 0, 0)$. Although the signal is coming towards us, we can, by optical reciprocity, solve the equation starting at $x = 0$ and following its path backwards.

Table 1: Parameters (with $1-\sigma$ errors) for the best $P(k)$ model of the WMAP1 normalized 2dFGRS data ($h = 0.7$). The form of the model is given by Eq. (1). Three exponentials were needed to fit the data.

a_i	a_i error	b_i (Mpc)	b_i error (Mpc)
0.883	0.17	128.0	11.0
0.114	0.02	39.3	3.80
0.0047	0.001	9.04	0.80

Suppose a signal arrives from a direction making a small angle $\boldsymbol{\theta}$ w.r.t. the x axis. This may correspond to some ‘off-axis’ point on the LSS in the case of the CMB. The conformal time of travel for our light signal is, from Eq. (6),

$$\eta = \int_0^x [1 - 2\Phi(x', \boldsymbol{\theta}x')]dx', \quad (7)$$

with an ensuing time delay of

$$\tau = \int_0^x 2\Phi(x', \boldsymbol{\theta}x')dx', \quad (8)$$

where x and x' can be present day physical distances if we set $a(z = 0) = a_0 = 1$ (here we ignored the geometric time delay, which is comparatively negligible as pointed out by HC01). Moreover, if we use the current value of Φ , as in the previous section, to calculate τ , then $\delta\tau = \delta t/a(t) = \delta t$. The ‘absolute’ variance of the time delay along a random direction $\boldsymbol{\theta}$ to the LSS

$$\langle \tau^2(\boldsymbol{\theta}) \rangle = \int_0^x 2dx' \int_0^x 2dx'' \langle \Phi(x', \boldsymbol{\theta}x')\Phi(x'', \boldsymbol{\theta}x'') \rangle, \quad (9)$$

is logarithmically divergent because the quantity $\langle \Phi(\mathbf{r})\Phi(\mathbf{r}') \rangle$ is, by Eq. (5), of the form $\int_0^k dk'/k'$ at small k . As stated in the beginning of the paper, HC01 renormalized $\langle \tau^2(\boldsymbol{\theta}) \rangle$ by subtracting an infinite constant from it.

Of more relevance to understanding the CMB acoustic peaks is the relative delay in the arrival time between the above signal and another light signal emitted simultaneously from the same distance, but along the ‘on-axis’ direction $\boldsymbol{\theta} = 0$, i.e.

$$\tau(\boldsymbol{\theta}) - \tau(\mathbf{0}) = \int_0^x 2x'\boldsymbol{\theta} \cdot \boldsymbol{\nabla}\Phi(x', \mathbf{0})dx' + \int_0^x x'^2(\boldsymbol{\theta} \cdot \boldsymbol{\nabla})^2\Phi(x', \mathbf{0})dx' + \dots, \quad (10)$$

where $\boldsymbol{\nabla}$ is the gradient operator transverse to the vector \mathbf{x} . assuming for the time being that the form of $P(k)$ is given by Eq. (A-4), we can construct the correlation function with the help of Eq. (5), as

$$\begin{aligned} \langle \nabla'_i \Phi(\mathbf{r}') \nabla''_j \Phi(\mathbf{r}'') \rangle &= \frac{(\delta\Phi)^2}{4\pi} \int \frac{d^3\mathbf{k}}{k^3} k_i k_j e^{i\mathbf{k} \cdot \mathbf{r}} e^{-bk} \\ &= \frac{(\delta\Phi)^2}{r^2} \left\{ \delta_{ij} \left[1 - \frac{b}{r} \arctan \left(\frac{r}{b} \right) \right] + \frac{r_i r_j}{r^2} \left[\frac{3b}{r} \arctan \left(\frac{r}{b} \right) - 2 - \frac{b^2}{r^2 + b^2} \right] \right\}, \end{aligned} \quad (11)$$

where

$$\mathbf{r} = \mathbf{r}' - \mathbf{r}'', \quad (12)$$

and the indices i, j denote *two* orthogonal components in directions transverse to x . This enables us to derive the lowest order term for the variance in the relative time delay $[\delta\tau(\theta)]^2 = \langle [\tau(\boldsymbol{\theta}) - \tau(\mathbf{0})]^2 \rangle$, viz. the first term on the right side of Eq. (10), as

$$[\delta\tau(\theta)]^2 = (\delta\Phi)^2 \boldsymbol{\theta}^2 \int_0^x 2x' dx' \int_0^x 2x'' dx'' \left[\frac{1}{r^2} - \frac{b}{r^3} \arctan\left(\frac{r}{b}\right) \right],$$

where $r = |x' - x''|$, consistent with Eq. (12).

Transforming now to the new variables $\bar{x} = (x' + x'')/2$ and $\tilde{x} = x' - x''$, the resulting integrand is symmetric in \tilde{x} , so we can restrict the range of \tilde{x} to positive values, introducing an extra factor of 2. Thus

$$\begin{aligned} [\delta\tau(\theta)]^2 &= 2(\delta\Phi)^2 \boldsymbol{\theta}^2 \int_0^x d\tilde{x} \int_{\frac{\tilde{x}}{2}}^{x - \frac{\tilde{x}}{2}} d\bar{x} \frac{4\bar{x}^2 - \tilde{x}^2}{\tilde{x}^2} \left[1 - \frac{b}{\tilde{x}} \arctan\left(\frac{\tilde{x}}{b}\right) \right] \\ &= \frac{4}{3}(\delta\Phi)^2 \boldsymbol{\theta}^2 \int_0^x d\tilde{x} \frac{2x^3 - 3x^2\tilde{x} + \tilde{x}^3}{\tilde{x}^2} \left[1 - \frac{b}{\tilde{x}} \arctan\left(\frac{\tilde{x}}{b}\right) \right]. \end{aligned} \quad (13)$$

By restricting ourselves to the limit $x \gg b$ ((appropriate to emission distances $x \gg b_1 \approx 0.1$ Mpc - see Table 1 - the CMB LSS clearly satisfies this criterion), it becomes straightforward to complete the calculation, because only one term stands out. The result is

$$[\delta\tau(\theta)]^2 = \frac{4}{3}(\delta\Phi)^2 \boldsymbol{\theta}^2 \frac{x^3}{b} \arctan\left(\frac{x}{b}\right) = \frac{2\pi}{3}(\delta\Phi)^2 \boldsymbol{\theta}^2 \frac{x^3}{b}. \quad (14)$$

Note that according to Eq. (14) the variation in the time delay difference between two points A and B on the LSS subtending an angle $\boldsymbol{\theta}$ at the observer O is $\delta\tau(\theta) \sim \theta$. This behavior indicates that we are in the regime of *coherent delay*, i.e. provided θ is sufficiently small the two rays sampled a primordial matter potential gradient which may be regarded as constant. Thus, if in Figure 2a a third point S_3 on the LSS is collinear with two other points S_1 and S_2 , then a constant gradient would imply equality between the ‘ S_1 to S_2 ’ and ‘ S_2 to S_3 ’ relative delays, i.e. both are $\delta\tau(\theta)$. Consequently the net S_1 to S_3 delay will be $2\delta\tau(\theta)$. Since the angular separation between S_1 and S_3 is $2\boldsymbol{\theta}$ at O, we have $\delta\tau(2\theta) = 2\delta\tau(\theta)$, fully consistent with the $\delta\tau(\theta) \sim \theta$ dependence.

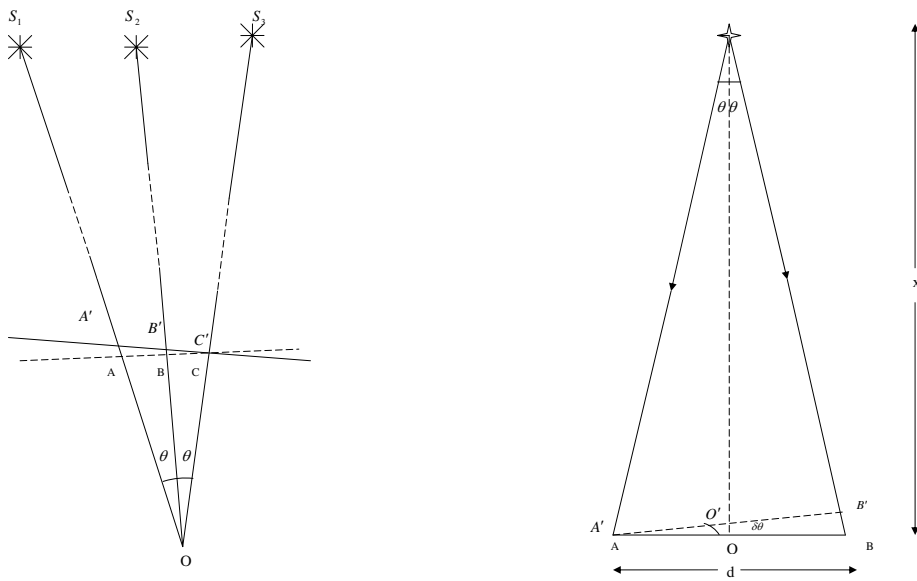


Fig. 2.— Illustrating the phenomenon of coherent time delay. 2a: simultaneously emitted light signals from three symmetrically located and equally distant sources would have arrived at points A, B, and C also at the same instance if there were no gravitational time delay. Provided θ is small enough that only the first spatial derivative of the potential is responsible for any delay, then the signals from S_1 and S_2 will e.g. have reached A' and B' when that from S_3 is at $C'=C$, where $AA'=2BB'$. The result is a net displacement of the angular position of all three sources by the same amount to the right. 2b: If we reverse the light paths by letting the observer be a single source and the former (S_1, S_2, S_3) be replaced by (B, O, A), then the source will appear shifted in the opposite direction (i.e. to the left) w.r.t. the observer whose telescope aperture is AB , as it should do.

Turning to the $\nabla^2\Phi$ term, which takes into account the difference in the potential gradient between the two rays, its exact mathematical form can be derived directly from the last integral of Eq. (10), but in this paper we will present instead another method of calculation which also provides unusual insights to the relationship between time delay and gravitational lensing. Such material is to be found in sections 4 and 5. For now we simply give the result, i.e. an expansion of $[\delta\tau(\theta)]^2$ to include the $\nabla^2\Phi$ term. It is

$$[\delta\tau(\boldsymbol{\theta})]^2 \approx \frac{2\pi}{3}(\delta\Phi)^2\theta^2\frac{x^3}{b}\left(1 - \frac{1}{20}\frac{x^2\theta^2}{b^2}\right) \text{ for } \theta < \theta_m; \quad (15)$$

or, if $P(k)$ has the more general form of Eq. (1), the contribution from the i th term to the variance (note the label i here has a *different* meaning from that in Eq. (11)) will be

$$[\delta\tau_i(\boldsymbol{\theta})]^2 \approx \frac{2\pi}{3}(\delta\Phi)^2\theta^2x^3\frac{a_i}{b_i}\left(1 - \frac{1}{20}\frac{x^2\theta^2}{b_i^2}\right) \text{ for } \theta < \theta_m^i, \quad (16)$$

where in Eqs. (15) and (16) the parameters θ_m and θ_m^i are yet to be defined below - see Eqs. (17) and (20). From Eq. (15) we see that the higher order (θ^4) term, once it assumes importance, will halt the linear rise of $\delta\tau(\theta)$ with θ . Eventually, when θ becomes large enough, all the higher order terms of Eq. (10) will take their place to ensure that $[\delta\tau(\theta)]^2$ reaches constancy¹, as it must do, because two widely separated rays are *uncorrelated*. Thus, once the θ^4 term is no longer negligible, *incoherence* takes over. A reasonable (and conservative) way of estimating the maximum (or ‘plateau’) value of $[\delta\tau(\theta)]^2$ is to find the angle at which the first θ -derivative of the right side of Eq. (15) vanishes. This occurs when

$$\theta_m = \sqrt{10}\frac{b}{x}, \quad (17)$$

at which point $\delta\tau$ reaches the constant (saturation) value of

$$[\delta\tau(\boldsymbol{\theta})]^2 = [\delta\tau(\theta_m)]^2 = \frac{10\pi}{3}(\delta\Phi)^2xb \text{ for } \theta \geq \theta_m \quad (18)$$

Here θ_m may be defined as the *coherence angle* for time delay. It is also closely related to the expansion parameter of the perturbation expansion of Eq. (15), because the ratio of the second order to the first order term of Eq. (15) is $2\theta_m^2$. When a more general form of $P(k)$, like Eq. (1), is considered, we have

$$[\delta\tau_i(\boldsymbol{\theta})]^2 = [\delta\tau_i(\theta_m^i)]^2 = \frac{10\pi}{3}(\delta\Phi)^2xa_i b_i \text{ for } \theta \geq \theta_m^i, \quad (19)$$

¹Strictly speaking there may be a gentle rise with θ because of the logarithmic divergence problem mentioned in section 1. This has no significant impact on any of the results presented in this paper, however.

where

$$\theta_m^i = \frac{\sqrt{10}b_i}{x} \quad (20)$$

for each component i of $P(k)$ in Eq. (1). The total variance of time delay is then the sum over i of all the individual variances $[\delta\tau_i(\boldsymbol{\theta})]^2$ as given by Eqs. (16) and (19). Obviously, for rays separated by angles $\theta > \theta_m$ the time delay is always completely incoherent (or random). As will be demonstrated in the next section, the significance of the transition angle θ_m is that for separation $\theta < \theta_m$, the variance for the coherent (or systematic) and incoherent delay is given by the first and second order terms of Eq. (15) respectively.

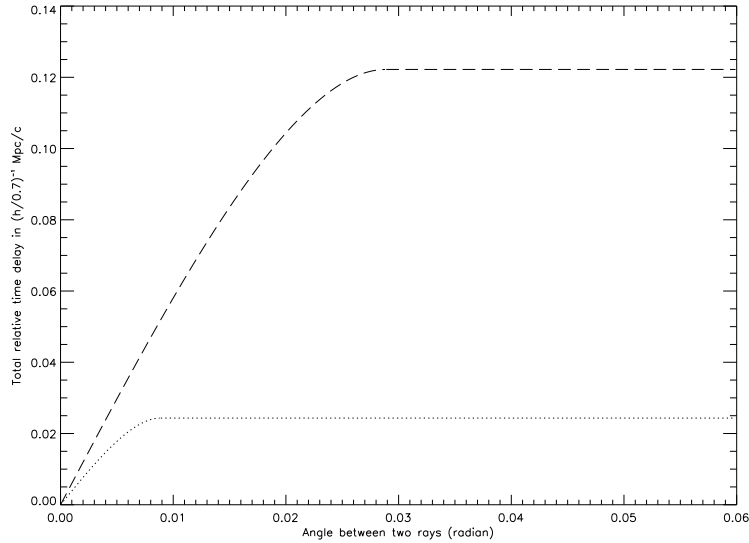


Fig. 3.— $1-\sigma$ relative time delay $\delta\tau^i(\theta)$ between two rays from the LSS due to the various terms i of primordial density perturbation of Eq. (1). In the limit $\theta \leq \theta_m^i$ where θ_m^i given by Eq. (20), $\delta\tau^i(\theta)$ is given by Eq. (16). When $\theta > \theta_m^i$, $\delta\tau^i(\theta)$ saturates to the value in Eq. (19). Long dashes correspond to the first term $i = 1$, and the dotted line to the second term $i = 2$ (the $i = 3$ term was ignored due to its insignificance). Values of a_i and b_i are shown in Table 1.

How does time delay affect CMB observations? When light signals emitted during the same redshift $z = z_{\text{LSS}}$ from two points on the LSS which subtend the angle θ at the observer are to arrive simultaneously *and yet* the times of flight are delayed w.r.t. each other, the signals would necessarily have covered different distances - the slower one must have undertaken a shorter journey. As illustrated in Figure 4, the consequence is a ‘tilt’ of the LSS in that vicinity. Hence, an angle θ which normally corresponds to an anisotropy on the LSS spanning the comoving distance $x\theta$ would now be randomly mapped to a *larger* distance $x(\theta + \delta\theta)$ where, from Figure 4,

$$\frac{\delta\theta}{\theta} = \frac{\delta\ell}{\ell} = \frac{[\delta\tau(\theta)]^2}{2x^2\theta^2} = \frac{1}{2x^2\theta^2} \sum_i [\delta\tau_i(\theta)]^2, \quad (21)$$

with the contribution to $(\delta\tau_i)^2$ from the i th term of Eq. (1) given by Eqs. (16) and (19). The net outcome is a *systematic* shift of the CMB acoustic peaks, which are features with fixed comoving scales, towards smaller angles or higher harmonic numbers ℓ .

It should be mentioned that another possible test of cosmological time delay concerns two light paths propagating through different parts of the Universe, but connecting the same source with the observer, i.e. a strong gravitational lensing scenario, under which multiple images occur. If this source undergoes flaring behavior, a time lag between the light curves of a pair of multiple images might result from perturbations in the distribution of primordial matter. In practice, however, this is a sensitive test only if the lowest order ($\delta\tau(\theta) \sim \theta$) term contributes to the delay. As it turns out, this term does *not* play a role because the potential time delay we have hitherto been considering is cancelled by another effect - the geometric delay - which *is* important under this scenario (see Bar-Kana 1996 and Seljak 1994). Since the higher order terms are too feeble to be measured, no meaningful constraints can be provided here.

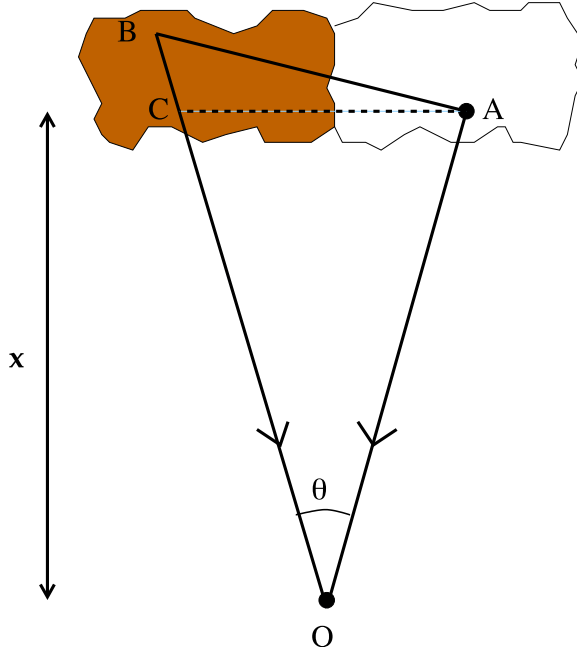


Fig. 4.— The effect of CMB time delay on the appearance of the acoustic peak hot and cold spots. Two proximity locations on the observed LSS are the points A and B. Were time delay absent, they would have been the points A and C. Here the distance BC is typically $\delta\tau(\theta)$, the quadrature sum (over all i) of the $\delta\tau_i(\theta)$ contributions as given by Eqs. (16) and (19), because it is the relative delay between the light signals emitted at A and C, with the path AO suffering from more delay than BO in this case. Since any LSS plane samples the same distribution of hot and cold spots as any other, the tilting of the LSS by time delay invariably means an observer charted slightly larger physical distance on the LSS for a certain angular separation between two temperature sensors. This *systematically* causes all acoustic peaks to move towards smaller θ , or larger ℓ , in the manner of Eq. (21).

4. Deflection angle fluctuation from primordial density contrasts

A significant gain in our general understanding of foreground effects is afforded by examining also the question of CMB lensing. In addition to the x -axis of section 3, which points along a radial direction from the observer's origin back to the LSS, we now introduce two more Cartesian (comoving) coordinates \mathbf{y} , both measuring distances transverse to the light path. Tracing the path towards the LSS as before, the equation of motion for a light signal is

$$\frac{d^2\mathbf{y}}{dx^2} = -2\nabla\Phi. \quad (22)$$

Let a signal arrive from some direction which makes a (small) angle $\boldsymbol{\theta}$ with the x axis. Then the solution to (28) is

$$\mathbf{y} = \boldsymbol{\theta}x + \delta\mathbf{y} = \boldsymbol{\theta}x - 2 \int_0^x dx' (x - x') \nabla\Phi(x', \boldsymbol{\theta}x'), \quad (23)$$

with appropriate initial conditions.

From Eq. (30) emerges that the correlation between the values of the deviation angle $\delta\mathbf{y}/x$ for different values of $\boldsymbol{\theta}$,

$$\begin{aligned} C_{ij}(|\boldsymbol{\theta}' - \boldsymbol{\theta}''|) &\equiv \frac{1}{x^2} \langle \delta y_i(\boldsymbol{\theta}') \delta y_j(\boldsymbol{\theta}'') \rangle \\ &= \frac{4}{x^2} \int_0^x dx' (x - x') \int_0^x dx'' (x - x'') \langle \nabla'_i \Phi(x', \boldsymbol{\theta}' x') \nabla''_j \Phi(x'', \boldsymbol{\theta}'' x'') \rangle. \end{aligned} \quad (24)$$

By means of Eqs. (24) and (11), one can expand the ensuing correlation function $C(\boldsymbol{\theta})$ as a Taylor series (see Appendix B for details on intermediate steps), i.e.

$$C(\boldsymbol{\theta}) = C_{ii}(\boldsymbol{\theta}) \equiv \frac{\langle \delta y_i(\frac{1}{2}\boldsymbol{\theta}) \delta y_i(-\frac{1}{2}\boldsymbol{\theta}) \rangle}{x^2} = \frac{4\pi}{3} (\delta\Phi)^2 \frac{x}{b} \left(1 - \frac{1}{20} \frac{x^2 \theta^2}{b^2} + \dots \right), \quad (25)$$

where the sum represented by a repeated index is over the two transverse dimensions.

5. Reciprocity of light propagation: the relationship between time delay and deflection

An interesting connection exists between sections 3 and 4, in that the key formulae derived in each section, viz. Eqs. (15) and (25), are closely related to each other because of a physical reason - the reciprocity of light propagation.

We first consider the scenario of a source S emitting light signals that enter an observer's circular telescope aperture at the extremities A and B such that the angle ASB is 2θ , see

Fig 2b. Let us assume that when the Universe is homogeneous, the wavefronts are parallel to the aperture as they arrive, i.e. the signals reach points A and B simultaneously. We further suppose that the same is true for two points C and D on the extremities of another aperture diameter perpendicular to the AB line - the source is ‘on-axis’.

In the presence of primordial matter density perturbation, let the signal propagating in the SB direction reach the point B’ when the SA signal has already arrived at A, i.e. the SA signal suffered from a smaller delay. The outcome is a tilting of the wavefronts as they enter the aperture - the source is now seen to have moved ‘off-axis’ along the AB line to a new position leftwards of the center O. The angle of tilt is $\delta\theta = 2\delta\tau(\theta)/d$ in the limit of coherent time delay (i.e. small θ) where $\delta\tau(\theta)$ is the distance BB’ and d is the diameter AB. Repeating our above argument to the points C and D, and noting that the relative delay between the SC and SD directions is *independent* of that between SA and SB, we realize that the variance

$$(\delta\boldsymbol{\theta})^2 = \frac{8[\delta\tau(\boldsymbol{\theta})]^2}{d^2} \quad (26)$$

applies to the overall shift in the position of the source on the two dimensional sky. Of particular interest is the fact that for a given source distance x the quantity

$$\theta = \frac{d}{2x} \sim d. \quad (27)$$

Thus, in order for the positional shift to be the same amount irrespective of aperture size d we must have $\delta\tau(\boldsymbol{\theta}) \sim \theta$ where $\theta^2 = \boldsymbol{\theta} \cdot \boldsymbol{\theta}$. From section 3 we saw that this condition holds only when θ , hence d , is small.

To link sections 3 and 4, however, we have to consider a second scenario, under which the distribution of primordial matter remains the same as before, but A, O, and B are now three simultaneously emitting sources and S is the observer (equipped with a small telescope). This reversal of the light paths converts Figure 2b into Figure 2a. By the reciprocity of light propagation, the signals must arrive at S in such a way that the change in the positions of the three sources as perceived by S after the ‘turning on’ of the matter perturbation involves an angular shift by the same amount $-\delta\boldsymbol{\theta}$ for each source. Yet according to section 4, this shift has a variance given precisely by the correlation function $C(\boldsymbol{\theta})$, where $\boldsymbol{\theta}$ is the angle the two sources subtend at the observer S, viz.

$$(\delta\boldsymbol{\theta})^2 = \frac{\langle \delta y_i(\frac{1}{2}\boldsymbol{\theta}) \delta y_i(-\frac{1}{2}\boldsymbol{\theta}) \rangle}{x^2} = C(\boldsymbol{\theta}), \quad (28)$$

with $C(\boldsymbol{\theta})$ being given by Eq. (25).

If we now take the limit $\theta \rightarrow 0$. By Eqs (28) and (22), the latter in section 4, we have

$$(\delta\boldsymbol{\theta})^2 = \frac{\langle \delta\mathbf{y}^2 \rangle}{x^2} = \frac{4\pi}{3}(\delta\Phi)^2 \frac{x}{b}, \quad (29)$$

which is a constant shift (of O w.r.t. A, and B w.r.t. O) independent of d and θ . Such a behavior is also consistent with the requirement stated at the end of the previous paragraph when we considered our first scenario. Thus, from Eqs. (26), (27), and (29) we deduce that

$$[\delta\tau(\theta)]^2 = \frac{2\pi}{3}(\delta\Phi)^2\boldsymbol{\theta}^2\frac{x^3}{b}, \quad (30)$$

which is the low θ limit of the variance in the relative time delay between two light paths separated by angle $\boldsymbol{\theta}$, as derived in Eq. (15) of section 3. Thus, it is now clear that sections 3 and 4 can be unified by the principle of light reciprocity.

Of even more interest, however, is the regime of larger θ , where incoherence between the two rays becomes important. Here we already saw from Eq. (25) of section 4 that $C(\boldsymbol{\theta})$, hence $(\delta\boldsymbol{\theta})^2$ by Eq. (28), is no longer a constant, but decreases away from constancy as θ increases. This decrease is expected, because when θ becomes sufficiently large the two light paths are independently perturbed by *different* primordial density fluctuations, i.e. the correlation function $\langle\delta y_i(\frac{1}{2}\boldsymbol{\theta})\delta y_i(-\frac{1}{2}\boldsymbol{\theta})\rangle$, hence $(\delta\boldsymbol{\theta})^2$ by Eq. (28), assumes relatively small values. The two sources shift their positions randomly w.r.t. each other, leaving behind little net systematic drift of their centroid across the sky (according to S). In fact, when we compare Eq. (25) in full with Eqs. (27) and (28), we obtain an expression for $[\delta\tau(\theta)]^2$ in complete agreement with Eq. (15). This consistency provided an important cross-check of the robustness of our analysis, and explains why the C_2 term in the variance represents incoherence effects - it is precisely this term that decorrelates $C(\boldsymbol{\theta})$. To labor upon this point even further, we observe that the variance of the *random relative deflection* between the two rays:

$$\frac{1}{x^2}\langle[\delta\mathbf{y}(\frac{1}{2}\boldsymbol{\theta}) - \delta\mathbf{y}(-\frac{1}{2}\boldsymbol{\theta})]^2\rangle = 2[C(0) - C(\boldsymbol{\theta})],$$

has the C_2 coefficient in is leading term. Thus, it is completely clear that while the C_0 coefficient concerns absolute deflection and coherent delay, the physics of C_2 is relative deflection and incoherent delay.

A word of caution, however, before we leave this section. Although the phenomena of time delay and deflection are two sides of the same coin, the ‘flipping of the coin’ involves reversing light path arrows, i.e. for a given set of arrows we should *not* conclude that delay presents no new physical effects than those ensuing from lensing. In particular, for the CMB which is emitted from a three dimensional distribution of sources, a varying time delay on simultaneously observed signals from different directions allows *depth* to play a role in the problem - as is already explained towards the end of section 3. This depth effect cannot be reproduced in any way by lensing.

6. Time delay distortion of the CMB acoustic peaks

We finally return to the original subject of this paper, viz. the degree to which time delay by foreground primordial matter re-processes the CMB primary anisotropy. In Eq. (1) and Table 1, we consider only the first two terms in our breakdown of density fluctuations, viz. $i = 1, 2$ of Eq. (1). Their coherence lengths are, by Eq. (20), $\theta_m^1 = \theta_1 = 0.0289$ or $\ell_1 = 108.8$, and $\theta_m^2 = \theta_2 = 0.00886$ or $\ell_2 = \pi/\theta_2 = 354.4$. Using Eq. (21), then, one derives the gaussian smoothing width of CMB anisotropy power, due to the $i = 1$ perturbation only, as

$$\frac{\delta\theta}{\theta} = 4.5 \times 10^{-8} \times (\delta\Phi/3 \times 10^{-5})^2 \times \begin{cases} \frac{\theta_1}{\theta}, & \theta > \theta_1, \\ 2(1 - 600\theta^2), & \theta < \theta_1. \end{cases} \quad (31)$$

Likewise one also derives the width due to the $i = 2$ term as

$$\frac{\delta\theta}{\theta} = 1.9 \times 10^{-8} \times (\delta\Phi/3 \times 10^{-5})^2 \times \begin{cases} \frac{\theta_2}{\theta}, & \theta > \theta_2, \\ 2(1 - 6363\theta^2), & \theta < \theta_2. \end{cases} \quad (32)$$

The total width $\delta\theta/\theta$ at a given θ is then the quadrature sum of the contributions (at that value of θ) from both the $i = 1$ and $i = 2$ terms, as in Eq. (21).

A graph of $\delta\ell/\ell = \delta\theta/\theta$ versus $\ell = \pi/\theta$ for the $i = 1$, $i = 2$ components and their total is shown in Figure 5. We explained in the end of section 3 that the smoothing kernel for $\delta\theta/\theta$ is a one-sided gaussian function in the case of time delay perturbations, i.e. structures on the LSS are invariably biased towards having smaller perceived angular sizes irrespective of how time delay may tilt the LSS. Specifically the kernel $K(\theta, \ell)$ that enters the integrand for the lensed CMB temperature correlation function, viz. Eq. (A5) of Seljak (1996) is

$$K(\theta, \ell) = \begin{cases} e^{-\ell^2\sigma^2(\theta)/2}, & \ell > \frac{\pi}{\theta}, \\ 0, & \ell < \frac{\pi}{\theta}, \end{cases} \quad (33)$$

where $0.6\sigma(\theta) = \delta\theta$ with $\delta\theta$ given by Eqs (31) and (32) added in quadrature, and the factor of 0.6 is due to the fact that the standard deviation of a one-sided gaussian having the usual form for its exponent has standard deviation 0.6σ .

Thus, after applying the (normal) simplifying procedures of Limber approximation and retention of only the isotropic term $J_0(\ell\theta)$ in Seljak's (A5), one arrives at the lensed correlation function due to time delay

$$\tilde{C}_\ell = \int_0^\pi \theta d\theta \int_0^\infty \ell d\ell K(\theta, \ell) C_\ell J_0(\ell\theta), \quad (34)$$

which is to be contrasted with Eq. (A7) of Seljak (1996). Owing to the smallness of the effect as dictated by the numerical coefficients in Eqs. (31) and (32), however, we did not

convolve the acoustic peaks according to the recipe of Eq. (34), because the distortion is completely unnoticeable². We can therefore corroborate HC01, after this comparatively more detailed and specific investigation (see section 1), by concluding that relative time delay by foreground primordial density fluctuations does not lead to any appreciable changes in the prediction of the standard cosmological model on the CMB acoustic anisotropy.

²In order for any smearing effects to distort the acoustic peaks to the point that the resulting standard cosmological model no longer matches WMAP3 data, it is necessary for $\sigma(\theta)/\theta$ to be at least 10 % at the center of the first peak.

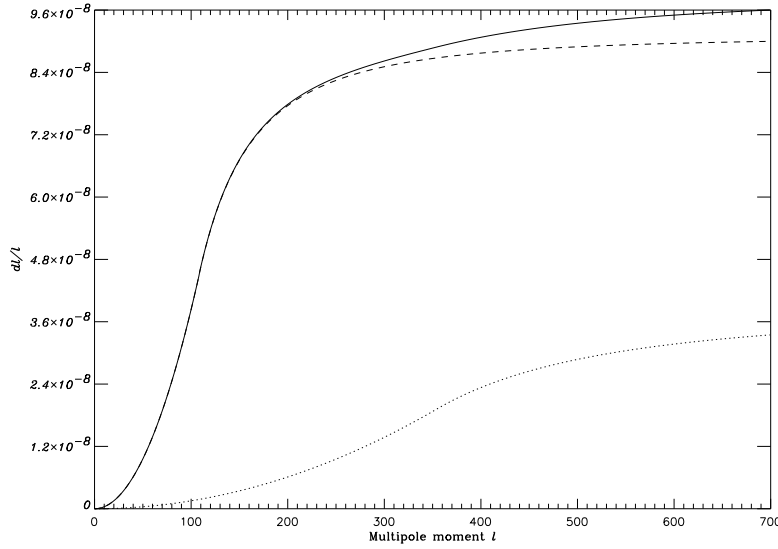


Fig. 5.— The percentage variation of the size of an acoustic harmonic ℓ due to time delay differences along the LSS, i.e. Eqs. (31) and (32), is plotted as a function of ℓ for contribution from the mode $i = 1$ (long dashes) and $i = 2$ (short dashes) of primordial density fluctuation in Eq. (1) and Table 1. The total $\delta\ell/\ell$ curve, obtained by adding the two dashed lines in quadrature, is shown as the solid line. Note that the $i = 3$ mode is ignored because of the smallness of its effect.

7. Can matter clumping affect the ‘mean’ geometry of space?

In spite of the feeble acoustic distortion induced by the time delay perturbation of the primordial matter distribution, its effect of biasing the acoustic peaks towards higher values of ℓ (as compared with the values under the scenario of a homogeneous Universe) remains in principle an interesting phenomenon. To illustrate, let us repeat the acoustic smearing computation in the previous section using a kernel $K(\theta, \ell)$ as determined by assuming a larger normalization of the matter power spectrum (than the WMAP value of Eq. (3)), viz.

$$\delta\Phi \approx 0.057. \quad (35)$$

The consequence, shown in Figure 6, is no longer negligible as before. The systematic shift of the acoustic peaks towards higher ℓ (or smaller θ) is now evident, and tends to force the best-fit model parameters to assume new values - that involve $\Omega < 1$ in particular. Thus clumping does not just introduce local fluctuations in the metric tensor (as first noted in section 3 of Einstein 1917), they *can* mimic space curvature, by altering the mean geometry of space as revealed by the statistical behavior of remotely emitted light along many and varied directions. The magnitude of this influence is by no means necessarily small: even the value of $\delta\Phi$ in Eq. (35) lies well within the perturbation criterion of $\delta\Phi \ll 1$, yet it led to a finite CMB $\delta\theta/\theta$ which, for the $i = 1$ term of Eq. (1), is *not* $\ll 1$ because it maximizes at 32.5 % when Eq. (31) is rescaled on the right side according to $\delta\theta/\theta \sim (\delta\Phi)^2$.

In the light of the above development, let us return to the question of why global space as measured by WMAP has zero curvature. It has widely been accepted that inflation solved the flatness problem, but does not answer why $\delta\Phi$ is as small as the value in Eq. (3), which implies an unusually weak scalar-field coupling. This view is still correct, so long as the ‘flatness’ is understood as an intrinsic rather than observed property of space, because indeed $\delta\Phi$, no matter what values it assumes, does not alter the mean intrinsic curvature. But since, as demonstrated in this work, even within the perturbation regime a larger $\delta\Phi$ can make an intrinsically flat geometry appear to WMAP as, on average, curved, then one must acknowledge that inflation has not explained why the *observed* mean curvature is zero.

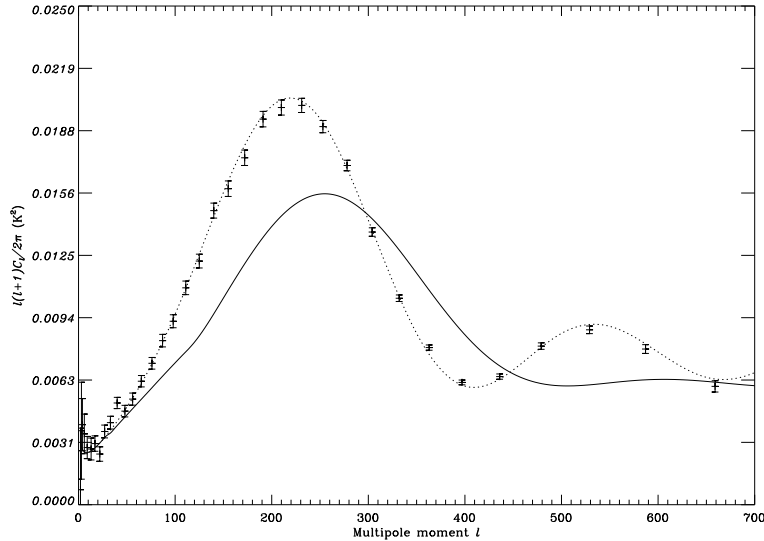


Fig. 6.— *Under the assumption* of an enhanced spectral normalization $\delta\Phi$ for the primordial density perturbation, i.e. with Eq. (35) replacing Eq. (3), the *rescaled* (hence *mock*) WMAP3 data and rescaled WMAP3 standard model prediction of the acoustic peaks are plotted, with the latter as a dotted line. This model is then re-processed by the lensed correlation function due to time delay, viz. Eq. (34) of section 5, again with the new $\delta\Phi$ value of Eq. (35).

The authors are grateful to Shaun Cole, Tom Kibble, Chris Kochanek, and an anonymous referee for their most helpful advice. RL thanks Esra Bulbul for the preparation of Figures 2, 4, and 7.

A. APPENDIX

The basic relationship between gravitational potential perturbation at various length scales and the matter power spectrum

During some epoch t , or redshift z , let the typical random excursion of the gravitational potential (from its mean value in a given cosmology) be Φ_k at wavenumber k or lengthscale $2\pi a/k$. By the Poisson equation, Φ_k is expressible in terms of the matter density variation $\delta_k(z) = \delta\rho_m^k(z)/\rho_m(z)$ as $\Phi_k = 4\pi G\rho_m(z)a^2\delta_k(z)/k^2$, where $a = a(t) = 1/(1+z)$ is the expansion factor. Squaring both sides, we obtain the variance Φ_k^2 , the additive nature of which enables us to write the equation in differential form, as

$$d\Phi_k^2 = [4\pi G\rho_m(z)]^2 a^4 \frac{d\delta_k^2}{k^4}. \quad (\text{A1})$$

Under a matter dominated scenario, $\delta_k \propto (1+z)^{-1} \propto a$, and since $\rho_m(z) = (1+z)^3\rho_m(0) = \rho_m(0)/a^3$, we see that $d\Phi_k^2$ is independent of epoch. Thus it may be written in terms of the present day quantities

$$d\Phi_k^2 = [4\pi G\rho_m(0)]^2 \frac{d\delta_k^2(0)}{k^4}, \quad (\text{A2})$$

where $d\delta_k^2(0)$ relates to the $z = 0$ matter power spectrum $P(k)$ as inferred from WMAP's standard model parameters (or, better still, the WMAP1/2dFGRS external correlation, see below) by

$$d\delta_k^2(0) = \frac{dk}{k} \frac{k^3 P(k)}{2\pi^2}. \quad (\text{A3})$$

It should be noted, however, that if vacuum energy (or dark energy) rather than matter dominates the low z Universe, Eq. (A-2) would have slightly overestimated the value of Φ_k at an earlier epoch.

Before proceeding further, therefore, we must estimate a strict limit on the inaccuracy of Eq. (A-2). Under a Λ -dominated scenario, the rapid expansion freezes the density distribution - the masses cannot move fast enough to counter it. As a result, δ_k tends to a constant independent of a (i.e. no further growth of density contrasts in the linear regime), and Φ_k decreases as a^{-1} . In a $\Omega_m = 0.3$, $\Omega_\Lambda = 0.7$, and $h = 0.7$ cosmology (Bennett et al 2003, Spergel et al 2007), vacuum domination occurs at about $z \approx 0.32$ (when $\Omega_m(1+z)^3 = \Omega_\Lambda$). Thus, between $z \approx 0.32$ and $z = 0$, $d\Phi_k$ decreased from its hitherto constant value by the

fraction $1 - a \approx 30\%$ (where a refers to the expansion factor at $z = 0.32$). It is clear then that any lightpath integrations of the potential from $z = 0$ back to some remote past (or vice versa) will certainly not lead to an overestimation of Φ_k by more than 20 % if ones uses Eq. (A-2) for Φ_k .

Let us *for the time being* suppose that the $z = 0$ matter power spectrum has the simple form

$$P(k) = A k e^{-bk}, \quad (\text{A4})$$

so that at small k the power spectrum takes the Harrison-Zel'dovich form $P(k) \sim k$. Then, assembling Eqs. (A-2) and (A-3), we have

$$d\Phi_k^2 = 8G^2 \rho_m^2 A e^{-bk} \frac{dk}{k} = (\delta\Phi)^2 A e^{-bk} \frac{dk}{k}, \quad (\text{A5})$$

where

$$(\delta\Phi)^2 = \lim_{k \rightarrow 0} \frac{d\Phi_k^2}{d\ln k} = \frac{9\Omega_m^2 H_0^4}{8\pi^2} A, \quad (\text{A6})$$

with H_0 being the Hubble constant and $c = 1$ here-and-after. At sufficiently large k , corresponding to wavelengths smaller than the size of the Universe (in today's distance scale) during matter-radiation equipartition, $P(k)$ cuts off because the modes could not grow. Thus, in the simple manner by which Eq. (A-4) depicted the matter spectrum, $b \sim 33$ Mpc, the equipartition horizon for a flat Universe with $h = 0.7$. The advantage of Eq. (A-4), as can be seen in sections 3 and 4, is that it affords us an analytical treatment of CMB foreground re-processing by primordial matter - time delay and lensing in particular - by a method of successive approximation from low to high orders which reveals unambiguously the coherent spatial scales of these effects.

B. APPENDIX

Angular correlation function of deflection due to primordial foreground matter

The correlation function $C(\boldsymbol{\theta})$ as defined by the first equality of Eq. (25), section 4, may be computed using Eqs. (24) and (11). We find

$$\begin{aligned} C(\boldsymbol{\theta}) = \frac{8(\delta\Phi)^2}{x^2} \int_0^x d\tilde{x} \int_{\frac{\tilde{x}}{2}}^{x - \frac{\tilde{x}}{2}} d\bar{x} \frac{(x - \bar{x})^2 - \frac{1}{4}\tilde{x}^2}{r^4} \\ \times \left[2r^2 - 2\bar{x}^2\theta^2 - \frac{b^2\tilde{x}^2\theta^2}{b^2 + r^2} + (3\bar{x}^2\theta^2 - 2r^2)\frac{b}{r} \arctan\left(\frac{r}{b}\right) \right], \end{aligned} \quad (\text{B1})$$

where $\bar{x} = (x' + x'')/2$, $\tilde{x} = x' - x''$ as in section 3, and

$$r^2 = \tilde{x}^2 + \bar{x}^2\theta^2. \quad (\text{B2})$$

because with the new x -variables we have, from Eq. (12), $\mathbf{r} = (\tilde{x}, \bar{x}\boldsymbol{\theta})$. By setting $\theta = 0$ one arrives at the variance of the deflection angle for a single light ray,

$$\begin{aligned} C_0 = C(0) = \frac{\langle \delta \mathbf{y}^2 \rangle}{x^2} &= \frac{8(\delta\Phi)^2}{x^2} \int_0^x d\tilde{x} \int_{\frac{\tilde{x}}{2}}^{x-\frac{\tilde{x}}{2}} d\bar{x} \frac{(x-\bar{x})^2 - \frac{1}{4}\tilde{x}^2}{\tilde{x}^4} \left[2\tilde{x}^2 - 2b\tilde{x} \arctan\left(\frac{\tilde{x}}{b}\right) \right] \\ &= \frac{8(\delta\Phi)^2}{3x^2} \int_0^x d\tilde{x} \frac{2x^3 - 3x^2\tilde{x} + \tilde{x}^3}{\tilde{x}^2} \left[1 - \frac{b}{\tilde{x}} \arctan\left(\frac{\tilde{x}}{b}\right) \right] \end{aligned} \quad (\text{B3})$$

Evaluating the integral yields

$$C_0 = C(0) = \frac{\langle \delta \mathbf{y}^2 \rangle}{x^2} \approx \frac{4\pi}{3}(\delta\Phi)^2 \frac{x}{b}, \quad (\text{B4})$$

in the limit $x \gg b$.

In general, the cross-correlation function $C(\theta)$ of Eq. (B-1) may be expanded as a Taylor series:

$$C(\boldsymbol{\theta}) = C_0 + \frac{1}{2}C_2\theta^2 + \mathcal{O}(\theta^4), \quad (\text{B5})$$

where

$$\begin{aligned} C_2 &= \left[\frac{d^2}{d\theta^2} C(\theta) \right]_{\theta=0} \\ &= \frac{32\delta\Phi^2}{x^2} \int_0^x d\tilde{x} \int_{\frac{\tilde{x}}{2}}^{x-\frac{\tilde{x}}{2}} d\bar{x} \frac{[(x-\bar{x})^2 - \frac{1}{4}\tilde{x}^2]\bar{x}^2}{\tilde{x}^4} \left[3\frac{b}{\tilde{x}} \arctan\frac{b}{\tilde{x}} - 2 - \frac{b^2}{\tilde{x}^2 + b^2} \right] \\ &= \frac{4\delta\Phi^2}{15x^2} \int_0^x d\tilde{x} \frac{4x^5 - 10x^3\tilde{x}^2 + 5x^2\tilde{x}^3 + \tilde{x}^5}{\tilde{x}^4} \left[3\frac{b}{\tilde{x}} \arctan\frac{b}{\tilde{x}} - 2 - \frac{b^2}{\tilde{x}^2 + b^2} \right]. \end{aligned} \quad (\text{B6})$$

Again as before, in the limit $x \gg b$ only the leading term needs to be kept. The result is

$$C_2 = -\frac{2\pi}{15}(\delta\Phi)^2 \left(\frac{x}{b}\right)^3. \quad (\text{B7})$$

We finally arrive at the expansion

$$C(\boldsymbol{\theta}) = \frac{\langle \delta y_i(\frac{1}{2}\boldsymbol{\theta}) \delta y_i(-\frac{1}{2}\boldsymbol{\theta}) \rangle}{x^2} = \frac{4\pi}{3}(\delta\Phi)^2 \frac{x}{b} \left(1 - \frac{1}{20} \frac{x^2\theta^2}{b^2} + \dots \right). \quad (\text{B8})$$

after substituting Eqs. (B-4) and (B-6) into Eq. (B-5).

REFERENCES

Bar-Kana, R., 1996, ApJ, 468, 17.

Bennett, C.L. et al 2003, ApJ, 148, 1.

Cole, S. et al 2005, MNRAS, 362, 505.

Efstathiou, G., Bond, J. R., and White, S. D. M. 1992, MNRAS, 258P, 1.

Einstein, A., 1917, S. -B. Preuss. Akad. Wiss., 142.

Hu, W., and Cooray A. 2001, PRD 63, 23504,

Lewis, A., and Challinor, A. 2006, PhR, 429, 1.

Peacock, J.A., 1999, Cosmological Physics, Cambridge University Press.

Sanchez, A.G., Baugh, C.M., Percival, W.J., Peacock, J.A., Padilla, N.D., Cole, S., Frenk, C.S., & Norberg, P. 2006, MNRAS, 366, 189.

Seljak, U. 1996, ApJ, 463, 1.

Seljak, U. 1994, ApJ, 436, 509.

Shanks, T. 2006, MNRAS submitted (astro-ph/0609339).

Spergel, D. et al, 2003, ApJS, 148, 175.

Spergel, D. et al, 2007, ApJ, in press (astro-ph/0603449).